Clinical Biomechanics 111 (2024) 106158

Contents lists available at ScienceDirect

Clinical Biomechanics

journal homepage: www.elsevier.com/locate/clinbiomech

ISB clinical biomechanics award winner 2023: Medial gastrocnemius muscle and Achilles tendon interplay during gait in cerebral palsy

Francesco Cenni [a,*], Nathalie Alexander [b], Maria Sukanen [a], Afet Mustafaoglu [a], Zhongzheng Wang [c], Ruoli Wang [c], Taija Finni [a]

[a] Faculty of Sport and Health Sciences, University of Jyväskylä, Jyväskylä, Finland
[b] Laboratory for Motion Analysis, Children's Hospital of Eastern Switzerland, St. Gallen, Switzerland
[c] KTH MoveAbility Lab, Department of Engineering Mechanics, KTH Royal Institute of Technology, Stockholm, Sweden

ARTICLE INFO

Keywords:
Muscle and tendon length
Fascicle length
Muscle and tendon strain
Pennation angle
Joint kinematics
Stance phase

ABSTRACT

Background: The interplay between the medial gastrocnemius muscle and the Achilles tendon is crucial for efficient walking. In cerebral palsy, muscle and tendon remodelling alters the role of contractile and elastic components. The aim was to investigate the length changes of medial gastrocnemius belly and fascicles, and Achilles tendon to understand their interplay to gait propulsion in individuals with cerebral palsy.
Methods: Twelve young individuals with cerebral palsy and 12 typically developed peers were assessed during multiple gait cycles using 3D gait analysis combined with a portable ultrasound device. By mapping ultrasound image locations into the shank reference frame, the medial gastrocnemius belly, fascicle, and Achilles tendon lengths were estimated throughout the gait cycle. Participants with cerebral palsy were classified into equinus and non-equinus groups based on their sagittal ankle kinematics.
Findings: In typically developed participants, the Achilles tendon undertook most of the muscle-tendon unit lengthening during stance, whereas in individuals with cerebral palsy, this lengthening was shared between the medial gastrocnemius belly and Achilles tendon, which was more evident in the equinus group. The lengthening behaviour of the medial gastrocnemius fascicles resembled that of the Achilles tendon in cerebral palsy.
Interpretation: The findings revealed similar length changes of the medial gastrocnemius fascicles and Achilles tendon, highlighting the enhanced role of the muscle in absorbing energy during stance in cerebral palsy. These results, together with the current knowledge of increased intramuscular stiffness, suggest the exploitation of intramuscular passive forces for such energy absorption.

1. Introduction

Accurate information on lower limb muscles and tendons during walking is essential to gain insight into the mechanical and energetic aspects of locomotion (Huang et al., 2015; Ishikawa et al., 2005; Orselli et al., 2018). Considering only the stance phase of gait, the ankle joint is particularly critical as it performs approximately 60% of the summed positive mechanical work of the ankle, knee, and hip (Sawicki et al., 2009). Therefore, most attention has been paid to the active force produced by contractile components of the calf muscles to power walking at the ankle level. Yet, walking is also supported by energy stored in elastic components, with the Achilles tendon (AT) absorbing energy during lengthening, thus enabling economical locomotion (Alexander, 1991; Sawicki et al., 2009). This optimal muscle-tendon interaction is altered in conditions where normal muscle function is impaired, such as in spastic cerebral palsy (CP) (Barber et al., 2017; Kalsi et al., 2016). To understand the adaptive mechanisms compromising efficient walking in CP, the contribution of contractile and elastic components acting at the ankle joint should be investigated.

Three-dimensional (3D) gait analysis traditionally relies on kinematics, kinetics and electromyography to infer muscle and tendon function indirectly. Muscle-tendon unit (MTU) lengths can be estimated based on musculoskeletal models (Kainz and Schwartz, 2021). However, a direct assessment of muscle and tendon lengths can be achieved by enhancing 3D gait analysis with an ultrasound device (3DGAUS) and tracking its probe (Cenni et al., 2021; Kalsi et al., 2016; Kharazi et al., 2021; Lichtwark and Wilson, 2006). This allows us to understand the efficacy of the interplay between muscle and tendon.

* Corresponding author at: Faculty of Sport and Health Sciences, University of Jyväskylä, Rautpohjankatu 8, 40700 Jyväskylä, Finland.
E-mail address: francesco.l.cenni@jyu.fi (F. Cenni).

https://doi.org/10.1016/j.clinbiomech.2023.106158
Received 14 August 2023; Accepted 29 November 2023
Available online 4 December 2023

Muscle-tendon interplay has mostly been assessed in healthy individuals, focusing on the triceps surae muscles due to their role in stability and propulsion during gait and their easy accessibility for imaging (Cronin and Lichtwark, 2013; Fukunaga et al., 2001). At a steady pace on a flat surface, the fascicles of the medial gastrocnemius (MG) muscle contract almost isometrically during single limb stance, whereas the AT acts like a spring to absorb energy during lengthening (Fukunaga et al., 2001; Lichtwark and Wilson, 2006). Such an uncoupling behaviour demonstrates that the MTU length changes are primarily associated with those of the series-elastic components (Monte et al., 2022). As the AT shortens during pre-swing, the release of its passive energy along with the concentric contraction of the MG fascicles contribute to forward propulsion via so-called catapult action (Ishikawa et al., 2005). In an optimally functioning system, this is the most energy efficient mechanism for walking (Sawicki et al., 2009).

In pathological conditions such as CP, musculoskeletal impairments often affect functional mobility. Intrinsic muscular changes may cause muscle contractures, along with the commonly accepted role of spasticity (Howard et al., 2022). In individuals with CP, plantarflexor muscles are not only shorter (relative to MTU length), but also smaller (relative to body mass) (Handsfield et al., 2022) and stiffer than in typically developing (TD) peers (Brandeburg et al., 2016; Lee et al., 2016). The reduced active force potential due to such muscle remodelling is further limited by alterations in neuronal activation (Stackhouse, 2005). This scenario, together with the fact that the AT is longer (Wren et al., 2010) and more compliant relative to the corresponding muscle (Theis et al., 2016), affects the efficiency of the muscle-tendon interplay.

Muscle-tendon interplay in CP is still poorly understood due to limited experimental data during gait. It has been reported that MG belly (Kalsi et al., 2016) and MG fascicle (Barber et al., 2017) work eccentrically during stance in equinus gait pattern (Horsch et al., 2022), but not in crouch (Hösl et al., 2016). This eccentric action appears to be caused by the incapacity of the MG to sustain an isometric contraction in the presence of external forces (Barber et al., 2017). However, the remodelled muscle properties together with the possible increase in the resting sarcomere length (Nikolaou et al., 2022; Smith et al., 2011) may be suboptimal for active force production (Harkness-Armstrong et al., 2021). When sarcomeres operate on the descending limb of the active force-length curve, the passive force-length curve has a substantial contribution which should be even larger in muscles of children with CP, considering the increased intramuscular stiffness (Lieber and Fridén, 2019). Therefore, it may be plausible to exploit the contribution of the elastic components via passive force transmission pathways within the muscle belly through connective tissue (Huijing, 1999). This could be achieved by absorbing energy also at the muscle level, thus sharing MTU lengthening between muscle and tendon during stance. Therefore, it is crucial to assess the contractile and elastic components independently to draw conclusions regarding the most efficient mechanisms in a remodelled muscle-tendon scenario.

For the first time within a single study, we experimentally assessed AT, MG fascicle and MG belly lengths during gait in young participants with CP, to distinguish the relative length changes of the contractile and elastic components. The first aim of this study was to quantify the differential contributions of MG belly and AT to the total MTU length changes during gait in participants with CP and their TD peers. We investigated whether in CP (especially for the participants walking with a reduced dorsiflexion, i.e., equinus gait pattern) the AT undertakes most of the MTU lengthening, as in TD participants, or whether the MG belly has a relevant contribution during the stance phase. The second aim was to understand the mechanisms occurring at the MG belly to facilitate its contribution to the MTU length changes in CP. We explored similarities between the behaviour of the MG fascicles and the AT, thus inferring about the recruitment of passive forces through stretch of the fascicles.

2. Methods

2.1. Subjects

Twelve individuals with CP (9 males, 3 females, 17.2 ± 4.2 years, Gross Motor Function Classification System: level $I = 8$, level III = 4) and 12 TD peers (9 males, 3 females, 16.8 ± 4.7 years) volunteered for this study. Participants were recruited from a previous EXECP-study (Valadão et al., 2021) and assessed at least 1.5 years after their last visit. The study was approved by the Research Ethics Committee of Central Finland Hospital District (Dnro 8 U/2017 amended 2021) and a written informed consent was acquired from participants and legal guardians of those under 18 years of age.

2.2. Protocol

Upon arrival to the laboratory, height (cm), body mass (kg) and tibia length (cm) were measured. Tibia length was measured between the center of the lateral condyle of the femur and the lateral malleolus. Passive ankle range of motion was manually measured using a goniometer, with the subject lying prone with the knee fully extended and the ankle in the following three joint positions: maximum tolerable dorsiflexion, maximum plantarflexion and the mid-range estimated from these two maxima. For the CP group, the most affected limb was measured, whereas for the TD participants a random limb was chosen. One operator placed 20 reflective markers on the body following the lower-limb Plug-in-Gait model (Kadaba, 2014) along with additional markers on the head of the fibula, tibial tuberosity and medial malleolus to define a local shank reference frame (Leardini et al., 2007). The ultrasound probe was attached to a probe holder instrumented with four reflective markers and secured to the leg using an elastic band, tight enough to provide a stable coupling with the leg but still limiting soft tissue deformation (Cenni et al., 2021). Next, participants were asked to walk along an 8-m walkway at self-selected speed. After a few minutes of habituation, a minimum of six trials were collected for each of the two conditions. In the first condition, the ultrasound probe was placed longitudinally over the distal MG muscle-tendon junction (MTJ), along the pulling direction of the AT. In the second condition, the ultrasound probe was placed over the MG mid-belly to image MG fascicles.

2.3. 3DGAUS acquisition

A 12-camera motion analysis system (Vicon Motion Systems Ltd., UK) operating at 200 Hz was synchronized with a portable ultrasound device (Telemed SmartUS, Lithuania) using a 60 mm linear probe to record images at 50 Hz. When necessary, participant-specific fine-tuning of the predefined US acquisition parameters (focus 17 mm, depth 65 mm, dynamic range 48 dB, power 0 dB, gain 60%, frequency 8 MHz) was performed to maximise visibility of the MTJ and MG fascicles. Data recording of the motion-analysis system was triggered from the ultrasound device using a voltage step signal. Nexus 2.12 (Vicon) and Echowave II 4.0 (Telemed) software were used. One operator carried the ultrasound device approximately 1.5 m behind the subject. Prior to each walking condition, static standing acquisitions were collected as reference values for the MG belly, MG fascicle, and AT lengths (video in supplementary material).

2.4. 3DGAUS processing

Ankle, knee and hip sagittal plane kinematics and gait events were estimated using the lower limb Plug-In Gait model, implemented by an automatic processing method (https://github.com/NCH-Motion-Laboratory/gaitutils). Data quality was monitored by an experienced operator. Joint kinematics and sole angles, i.e., the angle of the foot relative to the laboratory in the sagittal plane, were expressed over time-normalized gait cycles, based on the gait events. With respect to

overground gait, participants with CP were classified into two groups based on the mean ankle dorsiflexion in terminal stance: one group characterized by values that fell within the normal range of the TD data (CP non-equinus), and the other group with values below this range (CP equinus). Each CP participant's mean value during terminal stance was defined as decreased if it was below the control's mean ± one standard deviation. The two subgroups are hereinafter referred to as CP equinus and CP non-equinus.

The displacement of the MTJ as a single point was tracked using a semi-automatic algorithm validated for individuals with CP (Cenni et al., 2020). MG fascicle length was extracted semi-automatically as a straight-line distance between the superficial and deep aponeurosis, with one fascicle per image, and manual adjustments were made when necessary by checking every single image (Farris and Lichtwark, 2016). An open-source software (https://u0078867.gitlab.io/py3dfreeh andus/) was used to locate the ultrasound image in the shank reference frame (Cenni et al., 2016) and, in turn, the segmented MTJ and fascicle data (video in supplementary material). Absolute MG belly and AT lengths were defined as the Euclidean distance between the centre of the knee joint and the MTJ, and between the MTJ and the marker on the calcaneus, respectively, with the sum providing the total MTU length. The marker on the calcaneus was also virtually translated along the vertical direction, since the actual AT insertion was visualised and marked using ultrasound. The repeatability of the method has been previously established (Cenni et al., 2021).

From all the data processed, MG belly, MG fascicle and AT lengths were averaged over at least three time-normalized gait cycles per participant. Absolute lengths were normalized to the corresponding tibia lengths. Furthermore, absolute lengths at initial contact were subtracted to the corresponding values throughout the gait cycle and referred to as relative lengths (Barber et al., 2017). The reference lengths used to assess strains for MG belly, MG fascicle and AT were calculated when the participant was in a static standing position. In addition, the ratio of MG fascicle and MG belly, MG fascicle and AT, and MG belly and AT derived from absolute static standing lengths were calculated. Discrete mean values of joint kinematics, and MTU, MG belly, AT, and MG fascicle lengths (expressed as normalized, relative and strain) were averaged in single limb stance (Table 2) as well as in loading response and pre-swing (Table S2 in supplementary material), per group. The contribution of MG belly and AT to the overall MTU lengthening was expressed as ratio of MG belly to AT lengthening. The ratio was calculated individually throughout the gait cycle and expressed as values ranging from 0 to 1 (0 = no contribution to the MTU lengthening, while 1 = contribution to MTU lengthening comes entirely from one component). Negative and positive sign refer to shortening and lengthening, respectively. The same approach was applied to the interplay between MG fascicle and AT, and MG fascicle and MG belly, with the MG fascicle projected along the direction of the deep MG aponeurosis, by means of the corresponding pennation angle.

2.5. Statistics

Differences in group characteristics were identified using Kruskal-Wallis tests. In case of significance, post-hoc tests with Bonferroni correction were performed. For the discrete values in loading response, single limb stance and pre-swing between groups, the influence of walking speed was controlled by using ANCOVA. In case of significance, Tukey HSD post-hoc tests were performed on the fitted values. Effect sizes were quantified using Cohen's d (Cohen, 1992). The one-dimensional statistical parametric mapping (SPM) package (SnPM1D, www.spm1d.org) was used to compare waveforms using Python (Pataky, 2012). The SnPM test equivalent to a non-parametric ANOVA ($\alpha = 0.05$, with post-hoc Bonferroni-corrected non-parametric *t*-tests $\alpha = 0.017$) was used to compare gait, muscle and tendon parameters during the gait cycle. The coefficient of multiple correlation (CMC) was used to assess the similarity among the waveforms (Ferrari et al., 2010).

3. Results

No differences in age, height, body mass or tibia length were found among the groups (Table 1). CP equinus and CP non-equinus groups had significantly reduced passive maximum ankle dorsiflexion compared to the TD group. A significantly lower self-selected walking speed was found in CP equinus compared to the TD group. CP non-equinus group had a significantly smaller ratio between MG fascicle and MG belly in static standing compared to the TD group, whilst this reduction was not significant in CP equinus group.

The similarity of waveforms was assessed with CMC, showing muscle and tendon values above 0.715 in TD, while for CP the smallest values were 0.529 (Table S1 in supplementary material). Based on gait analysis, 6 participants were categorized as CP equinus and 6 as CP non-equinus (Fig. 1). For TD, kinematic data were only available for 11 participants due to a missing marker. By looking at the discrete values (Table 2), the mean sagittal ankle angles in single limb stance showed reduced dorsiflexion for the CP equinus group, and, conversely, an excessive dorsiflexion for the non-equinus group, compared to the TD group, with differences between the CP groups. For the CP equinus group, differences compared to the TD group were found for sole angle at the loading response (Table S2) and in single limb stance, with a flat initial contact of the foot instead of a heel strike.

Comparing waveforms during stance, the CP equinus group had significantly shorter MTU lengths (1.0 ± 0.1) compared to the TD group (1.1 ± 0.1) (Fig. 2). This comparison was not confirmed by the corresponding average value with a large effect size (Table 2). Normalized AT lengths were similar among groups (Fig. 2). Relative AT lengths for CP groups showed a rapid increase of lengthening at loading response phase compared to the TD group (5.9 ± 1.9 mm for CP non-equinus with large effect size and 4.0 ± 2.4 mm for CP equinus with small effect size), whilst TD group had 2.9 ± 2.2 mm of increase within the same time interval (Table 2).

Overall, normalized MG fascicle lengths were shorter in both CP groups than in TD (Fig. 2 and Table 2), throughout single limb stance. Although not significant, pennation angle at pre-swing was larger in CP equinus than TD group, with a large effect size (Table S2). A significant difference for the relative MG fascicle length at pre-swing was found between CP groups, and for CP non-equinus compared to the TD group (Table S2).

The TD group showed a shared contribution between the MG belly and AT to the overall MTU length changes at the loading response (Fig. 3). During single limb stance, at 40% of the gait cycle, the AT was the main contributor to length changes with an 80% share, while in pre-swing the scenario was similar to the one observed at the loading response (Fig. 3). For CP non-equinus, the AT contribution tended to decrease throughout single limb stance contributing about 60% of the MTU length change. For CP equinus, MTU length changes were shared almost equally between MG belly and AT.

Comparing MG fascicles and AT interplay for the TD group, AT had the predominant effect in single limb stance (71%), while MG fascicle started to take over at the end of push-off (Fig. 4). In CP non-equinus there was an even larger contribution of the AT in single limb stance (92% as maximum value), while the MG fascicles contribution increased towards the swing phase. This pattern was not observed in CP equinus, who showed a shared lengthening of these two components after loading response. In CP equinus, MG fascicle resembled the AT pattern during loading response and single limb stance phase, with a similar MG fascicle shortening at pre-swing compared to the other groups. The interplay between MG fascicle and MG belly is presented in Fig. S1.

4. Discussion

This study combined traditional gait analysis with ultrasound to experimentally and independently estimate the MG belly, MG fascicles and AT lengths during gait. The findings addressed the contribution of

Table 1
Group characteristics. Mean ± standard deviations are presented for each group, along with *p* values from Kruskal-Wallis test and effect sizes using Cohen's d. Post-hoc tests are presented in case of significance in the Kruskal-Wallis test and difference compared to the TD group (#) and between CP groups (*) at $p < 0.05$ are denoted.

	TD ($n = 12$)	CP eq ($n = 6$)	CP non-eq ($n = 6$)	P value Kruskal-Wallis	Cohen's d (TD – CP eq)	Cohen's d (TD – CP non-eq)	Cohen's d (CP eq – CP non-eq)
Age [years]	16.8 ± 4.7	17.7 ± 5.0	16.7 ± 3.4	0.915	−0.172	0.038	0.231
Height [cm]	167.4 ± 11.6	165.9 ± 9.8	164.8 ± 8.5	0.905	0.132	0.237	0.118
Body mass [kg]	63.7 ± 13.1	55.6 ± 11.0	58.9 ± 14.7	0.379	0.647	0.350	−0.254
Tibia length [cm]	39.8 ± 3.3	41.6 ± 5.1	39.6 ± 2.1	0.845	−0.461	0.056	0.507
Passive max dorsiflexion [deg]	12.9 ± 5.0	−5.0 ± 6.3 #	1.7 ± 9.3 #	**0.001**	3.296	1.693	−0.838
Passive mid-range of motion [deg]	−21.2 ± 4.8	−24.2 ± 4.9	−20.8 ± 4.9	0.362	0.601	−0.086	−0.678
Passive max plantarflexion [deg]	−45.0 ± 6.0	−43.3 ± 5.1	−39.2 ± 4.9	0.141	−0.289	−1.022	−0.826
Walking speed [m/s]	1.4 ± 0.2	0.9 ± 0.2 #	1.3 ± 0.3	**0.037**	2.276	0.658	−0.894
MG fascicle/MG belly in standing	0.22 ± 0.01	0.20 ± 0.04	0.17 ± 0.03 #	**0.010**	0.998	2.295	0.736
MG fascicle/AT in standing	0.30 ± 0.06	0.23 ± 0.10	0.24 ± 0.11	0.129	0.995	0.910	−0.045
MG belly/AT in standing	1.37 ± 0.30	1.13 ± 0.39	1.34 ± 0.44	0.445	0.725	0.093	−0.495

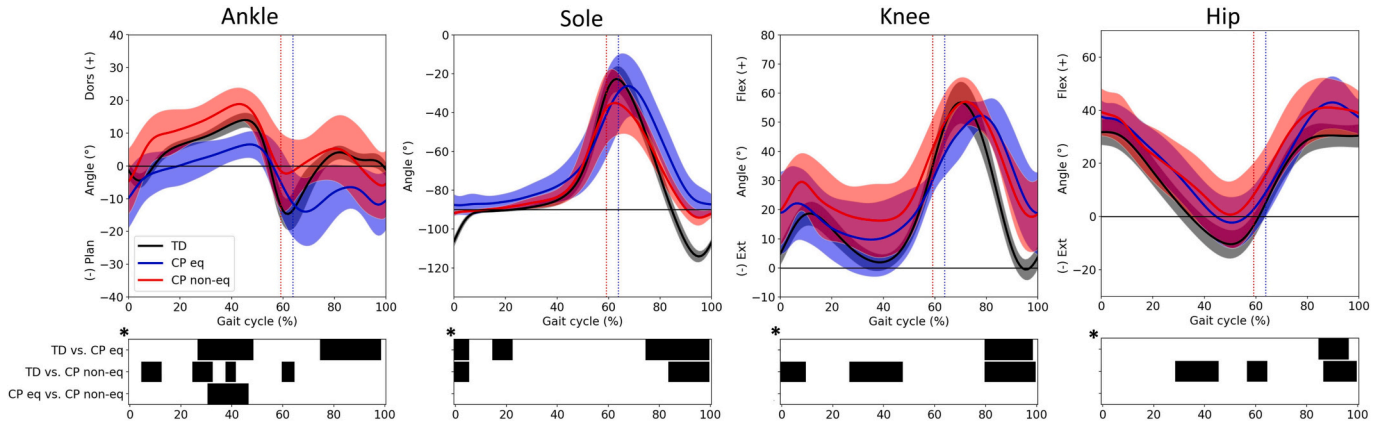

Fig. 1. Mean and standard deviation of the ankle, knee and hip angles in the sagittal plane, and sole angle, for the TD (grey), CP equinus (blue) and CP non-equinus (red) groups during the gait cycle. Vertical lines separate stance (from 0% initial contact) from swing phase (from approximately 60% to 100%). Bottom panel with * shows a significant ANOVA. Bottom panel with black horizontal bars shows times of the gait cycle where the groups differed significantly at $p < 0.017$, considering Bonferroni correction. (For interpretation of the references to colour in this figure legend, the reader is referred to the web version of this article.)

MG belly and AT to the relative MTU length changes during gait, highlighting the enhanced action of the MG belly in absorbing energy during stance in individuals with CP. By extending the analysis towards the role of the MG fascicles, we showed that longer operating length especially in CP equinus gait may take advantage of passive forces during stance, considering the knowledge of increased intramuscular stiffness (Lieber and Fridén, 2019; Smith et al., 2011).

Our first aim was to quantify the contribution of MG belly and AT to the relative MTU length changes during the gait cycle. A lengthening behaviour for both MG belly and AT during stance was shown in CP participants, which was particularly evident in the CP equinus (Fig. 3). In contrast, for TD participants, lengthening of the AT during single limb stance confirmed its main role in absorbing energy during that phase of the gait cycle (Fukunaga et al., 2001; Lichtwark and Wilson, 2006). Similar considerations could be inferred by looking at the lengths of the MTU, MG belly and AT during stance in TD. In agreement with previous studies (Barber et al., 2017; Kalsi et al., 2016), we showed an increase of the relative MTU lengths in CP, although only in the non-equinus group (Table 2, Fig. 2). The simultaneous relative AT lengths were similar among groups, thus the increase of MTU lengths seems to be dictated by the eccentric action of the MG belly in single limb stance (Barber et al., 2017). In addition, by looking at the relative AT lengths in Fig. 2, the CP groups showed lengthening starting from the initial contact followed by a nearly isometric pattern until the terminal stance phase. Thus, the AT has almost fully utilised its full capacity to store energy at the beginning of the gait cycle, suggesting the need for a mechanism at muscle level to store energy throughout the single limb stance.

The calculated relative AT lengths were comparable to a similar experimental approach (Kalsi et al., 2016), where the length was measured between MTJ and calcaneal insertion. Previously, larger relative AT lengths were reported when the length was estimated by subtracting the longitudinally projected MG fascicle length from the MTU (Barber et al., 2017). The latter method can result in over-estimation of tendon length changes and strain since the projection of a single fascicle for the MG underestimates the whole muscle belly length, and it does not take into account additional aponeurosis tissue included in the measure of AT (Finni et al., 2022).

The second aim was to understand the mechanisms within the MG belly that facilitate its contribution to the MTU length changes in individuals with CP. We showed that the behaviour of MG fascicles resembled the AT pattern, thereby suggesting that fascicles exploit more their passive rather than active forces during stance in the CP equinus group (Fig. 4). MG fascicles seem to utilize their passive elasticity while operating at longer lengths compared to TD. This may be due to the

Table 2
Joint kinematics, and muscle-tendon unit lengths averaged in single limb stance. Mean ± standard deviations are presented for each group, along with p values from ANCOVA test and effect sizes using Cohen's d sizes (defined as small (d = 0.20–0.49), medium (d = 0.50–0.79) or large (d > 0.80)). Difference compared to the TD group (#) and between CP groups (*) at $p < 0.05$ are denoted.

Variables in single limb stance	TD (n = 11)	CP eq (n = 6)	CP non-eq (n = 6)	P value ANCOVA	Cohen's d (TD – CP eq)	Cohen's d (TD – CP non-eq)	Cohen's d (CP eq – CP non-eq)
Sagittal ankle angle [°]	8.5 ± 1.2	2.7 ± 4.0*#	14.0 ± 5.1*#	**0.000**	2.118	−1.617	−2.250
Sole angle [°]	−87.7 ± 1.2	−80.4 ± 7.4 *#	−86.2 ± 2.1 *#	**0.039**	−1.501	−0.877	0.968
Sagittal knee angle [°]	8.7 ± 3.0	13.4 ± 10.2	19.5 ± 10.0	0.083	−0.671	−1.585	−0.555
Sagittal hip angle [°]	7.8 ± 4.5	14.2 ± 6.4	17.2 ± 9.6	0.100	−1.147	−1.305	−0.329
normalized MTU length [ ]	1.1 ± 0.1	1.0 ± 0.1	1.1 ± 0.1	0.135	1.316	0.065	−1.273
relative MTU length [mm]	3.9 ± 2.2	4.8 ± 5.6 *	11.4 ± 5.8 *#	**0.008**	−0.215	−1.860	−1.071
MTU strain [%]	0.7 ± 2.0	−0.3 ± 1.2	2.2 ± 3.1	0.151	0.520	−0.609	−0.980
normalized MG belly length [ ]	0.6 ± 0.1	0.5 ± 0.1	0.6 ± 0.1	0.186	1.613	0.028	−1.403
relative MG belly length [mm]	0.2 ± 1.7	−0.7 ± 4.4	4.1 ± 3.9	0.065	0.302	−1.383	−1.048
MG belly strain [%]	1.8 ± 3.5	−1.9 ± 3.8 *#	6.2 ± 6.7 *#	**0.003**	0.981	−0.857	−1.361
normalized AT length [ ]	0.5 ± 0.1	0.5 ± 0.1	0.5 ± 0.1	0.757	−0.325	−0.016	0.263
relative AT length [mm]	4.1 ± 2.6	4.6 ± 2.8	6.5 ± 2.3	0.092	−0.199	−0.933	−0.675
AT strain [%]	0.8 ± 6.1	3.2 ± 2.6	0.1 ± 2.6	0.287	−0.426	0.137	1.100
normalized MG fascicle length [ ]	0.1 ± 0.0	0.1 ± 0.0 #	0.1 ± 0.0 #	**0.034**	1.549	1.979	0.249
MG pennation angle [°]	14.4 ± 2.6	17.2 ± 5.3	16.8 ± 5.1	0.209	−0.714	−0.618	0.076
relative MG fascicle length [mm]	−1.9 ± 2.2	0.9 ± 2.6	1.0 ± 0.9	0.065	−1.120	−1.454	−0.065
MG fascicle strain [%]	−2.6 ± 7.3	−0.8 ± 6.0	−7.0 ± 13.3	0.267	−0.247	0.426	0.548

inability of the participants with CP to produce active force to sustain an isometric contraction. Considering that the muscle remodelling in CP includes an increase of passive muscle stiffness (Brandeburg et al., 2016), the amount of extracellular matrix-based collagen may be exploited to support a substantial portion of the load applied to the muscle belly (Howard et al., 2022). This scenario suggests a compensation of the lack of active forces with an enhanced pathway for passive muscular force transmission (Huijing, 1999). Furthermore, this highlights the need to separately analyses muscle belly and fascicles, since they provide different information, especially in pathological conditions.

For the MG fascicle, we observed shorter lengths (when normalized to tibia length) in CP than in TD individuals (Hösl et al., 2016) (Fig. 2). Relative MG fascicle lengths in CP showed a similar pattern as in a previous study, with a slight eccentric behaviour during stance and a reduced shortening at push-off compared to the TD group (Barber et al., 2017). During swing phase, the MG fascicles of TD reach the shortest length while CP equinus and especially CP non-equinus shorten, but to a smaller extent (Fig. 2). Such reduced shortening action is probably compensated by shorter MG fascicle length (relative to the AT) in CP compared to the TD group (Table 1). The smaller this ratio, the greater the overall effect of AT compliance on the MTU (Lieber and Fridén, 2019), hence facilitating sarcomere shortening. Furthermore, in proportion to MG belly, we found that MG fascicles were longer in the CP equinus than in the non-equinus group in static standing (Table 1). Similar results were reported also for idiopathic toe-walking, suggesting that higher force capability might be produced at longer fascicle lengths (Harkness-Armstrong et al., 2021). Assuming a similar capacity for myofiber growth and regeneration in skeletal muscle for both CP groups, such longer fascicles might be a consequence of overstretched sarcomeres. This together with the increased intramuscular stiffness in CP cannot only be thought of as driving factor for muscle weakness in CP, but also as a medium to enhance passive force transmission.

This study has some limitations. Wearing an ultrasound probe might cause gait alteration, although a recent study has reported minimal kinematic changes (Mooijekind et al., 2023). The pennation angle was measured assuming that the probe surface was parallel to the deep aponeurosis. This was not always the case, although an error of maximum 8° was estimated, corresponding for the longitudinal fascicle projection of an error approximately <6% in length. The ratio introduced in Figs. 3 and 4 is prone to high variability at the extreme of the gait cycle where the relative lengths used are close to zero. Yet, this does not affect the considerations made for the stance phase. Muscle activation was not reported for this study, therefore concentric and eccentric actions can only be inferred based on previous studies including electromyography. The 3DGAUS technique applied in this study was validated only in healthy condition (Cenni et al., 2021), therefore this should also be investigated in CP, where ultrasound image quality does not always allow a clear identification of fascicles and MTJ (supplementary material). This study did not account for AT curvature (Tecchio et al., 2022), and it may have resulted in about 1% error when estimating AT lengths. By analysing relative change in length, we have inferred about forces, as we have known since the pioneering work of Blix and Hill (Blix, 1892). However, we could not directly measure the forces produced by skeletal muscles, and future developments enabling to measure individual muscle forces will promote new frontiers in biomechanics (Dick and Hug, 2023). Furthermore, it would be useful to include data about muscle and tendon stiffness to better address considerations on force transmissions. Finally, we have analysed a limited number of participants, hence we have included effect size for a better interpretation of the statistical analysis.

5. Conclusion

We experimentally assessed changes in MG belly, MG fascicles and AT length in individuals with CP and TD peers during gait. The AT undertook most of the MTU lengthening in TD participants in stance, whereas in CP such lengthening was shared between the MG belly and AT, particularly in the CP equinus group. This suggested the role of the MG belly in absorbing energy during stance. Behaviour of the MG fascicles resembled the pattern of AT during stance. This may reflect muscle's inability to contract and produce force, and the need of muscle-tendon unit to rely more on passive tissues for absorbing energy during gait in CP.

Supplementary data to this article can be found online at https://doi.org/10.1016/j.clinbiomech.2023.106158.

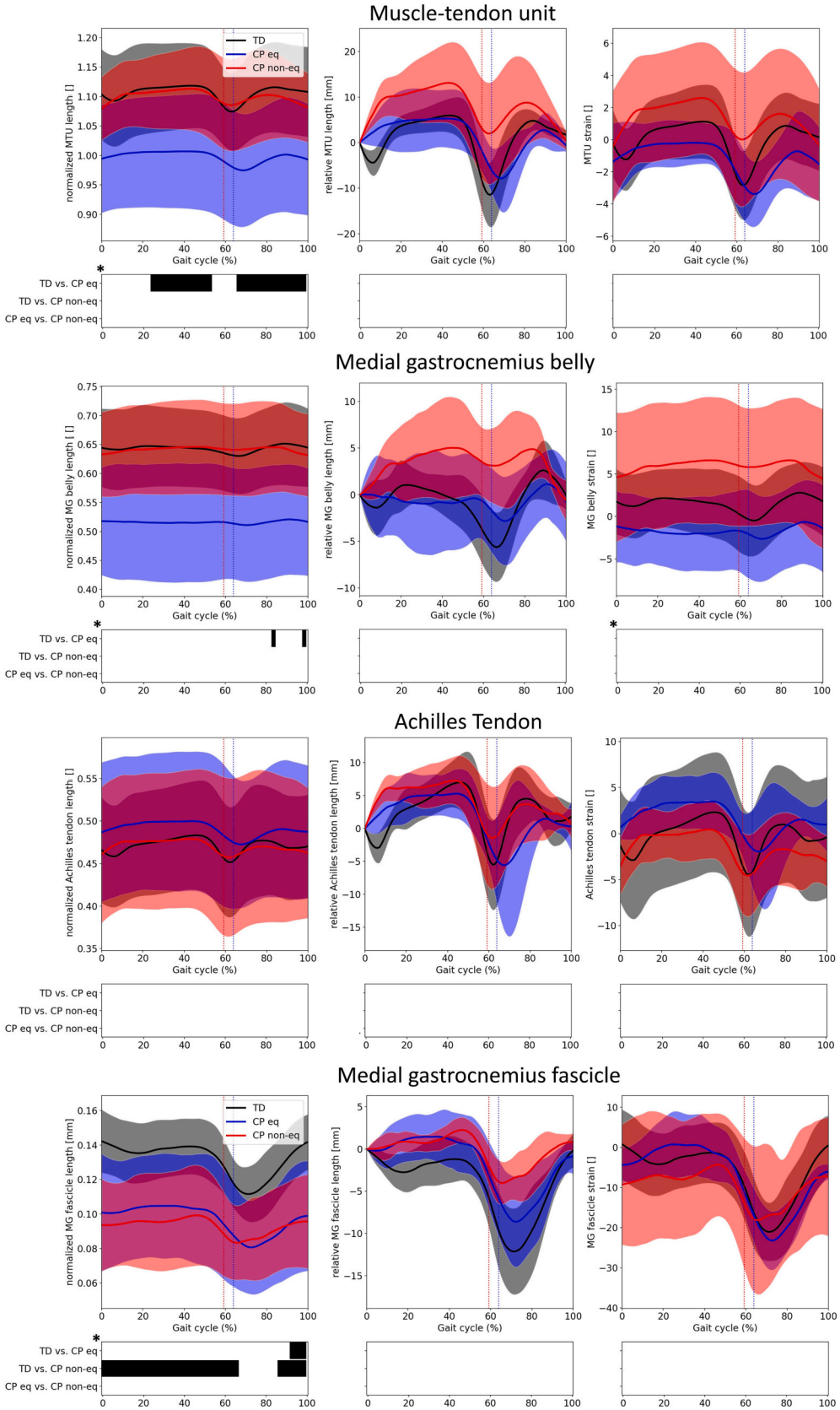

Fig. 2. For each row, mean and standard deviation of normalized lengths (left), relative lengths (middle) and strain (right) are displayed, whilst columns show muscle-tendon unit, medial gastrocnemius belly, Achilles tendon and medial gastrocnemius fascicle, respectively, for TD (grey), CP equinus (blue) and CP non-equinus (red) groups during gait cycle. Vertical lines separate stance (from 0% initial contact) from swing phase (from approximately 60% to 100%). Bottom panel with * shows a significant ANOVA. Bottom panel with black horizontal bars shows times of the gait cycle where the groups differed significantly at $p < 0.017$, considering Bonferroni correction. (For interpretation of the references to colour in this figure legend, the reader is referred to the web version of this article.)

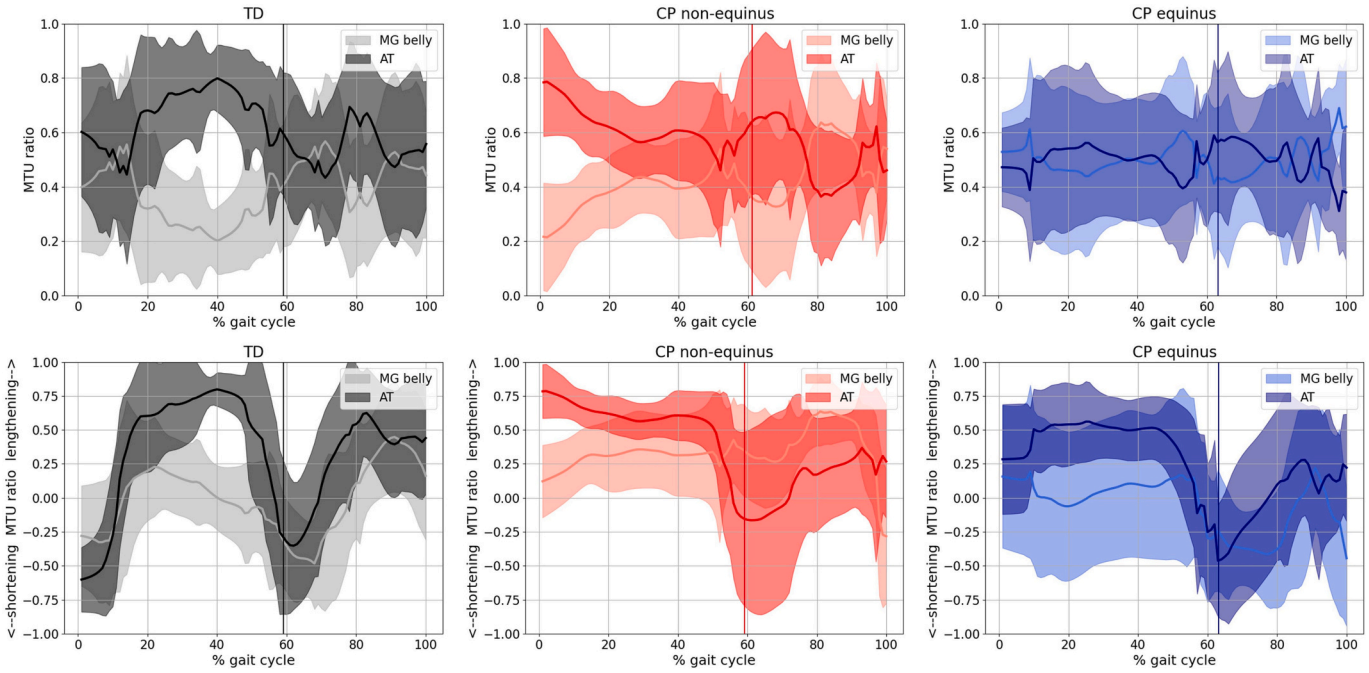

Fig. 3. Mean and standard deviation of the relative MG belly (lighter colour) and AT (darker colour) contribution to the overall MTU length change over the gait cycle. This ratio is reported as absolute values (first row), and as shortening (negative sign) and lengthening (positive sign) contributions (second row). Columns show TD group (grey), CP non-equinus (red) and CP equinus (blue), respectively. Vertical lines separate stance (from 0% initial contact) from swing phase (from approximately 60% to 100%). (For interpretation of the references to colour in this figure legend, the reader is referred to the web version of this article.)

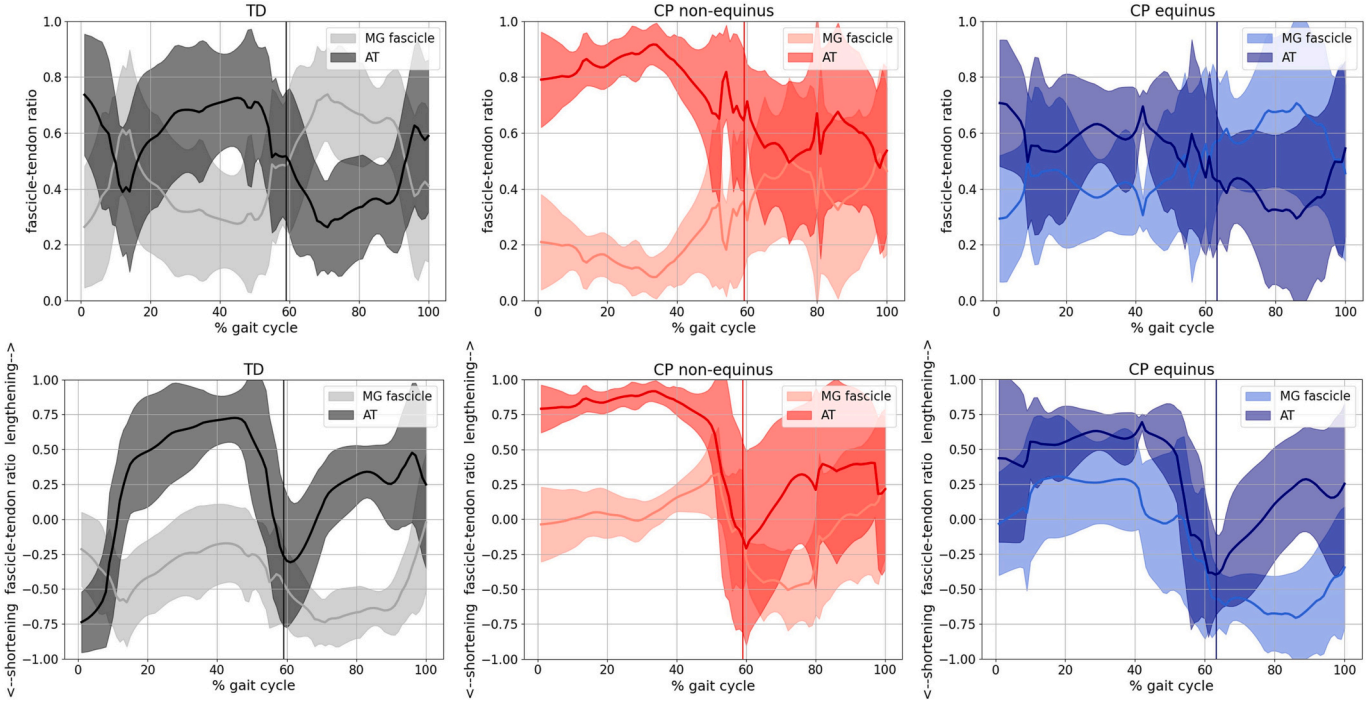

Fig. 4. Mean and standard deviation of the relative MG fascicle (lighter colour) and AT (darker colour) contribution to the overall MTU length change over the gait cycle. This ratio is reported as absolute values (first row), and as shortening (negative sign) and lengthening (positive sign) contributions (second row). Columns show TD group (grey), CP non-equinus (red) and CP equinus (blue), respectively. Vertical lines separate stance (from 0% initial contact) from swing phase (from approximately 60% to 100%). (For interpretation of the references to colour in this figure legend, the reader is referred to the web version of this article.)

Funding

Francesco Cenni is funded by the Marie Sklodowska-Curie, grant agreement No 101028724, and Promobilia No 20040.

Declaration of Competing Interest

None.

Acknowledgements

The authors like to thank Iida Laatikainen-Raussi, Dr. Marije Goudriaan, Alessandra Arthemalle and Lisa Dolci for the support provided during the measurement sessions. Furthermore, we are grateful to Dr. Juha-Pekka Kulmala and Jussi Nurminen for the guidance in the usage of the software for automatically processing gait analysis data.

References

Alexander, R.M., 1991. Energy-saving mechanisms in walking and running. J. Exp. Biol. 160, 55–69. https://doi.org/10.1242/jeb.160.1.55.

Barber, L., Carty, C., Modenese, L., Walsh, J., Boyd, R., Lichtwark, G., 2017. Medial gastrocnemius and soleus muscle-tendon unit, fascicle, and tendon interaction during walking in children with cerebral palsy. Dev. Med. Child Neurol. 59, 843–851.

Blix, M., 1892. Die Länge und die Spannung des Muskels.

Brandeburg, J., Eby, S.F., Song, P., Bamlet, W., Sieck, G.C., 2016. Quantifying passive muscle stiffness in children with and without cerebral palsy using ultrasound shear wave elastography. https://doi.org/10.1111/dmcn.13179.

Cenni, F., Monari, D., Desloovere, K., Aertbeliën, E., Schless, S.-H., Bruyninckx, H., 2016. The reliability and validity of a clinical 3D freehand ultrasound system. Comput. Methods Prog. Biomed. 136.

Cenni, F., Bar-On, L., Monari, D., Schless, S.H., Kalkman, B.M., Aertbeliën, E., Desloovere, K., Bruyninckx, H., 2020. Semi-automatic methods for tracking the medial gastrocnemius muscle–tendon junction using ultrasound: a validation study. Exp. Physiol. 105, 120–131. https://doi.org/10.1113/EP088133.

Cenni, F., Schless, S.H., Adams, H., Bar-On, L., Desloovere, K., 2021. The reliability of measuring medial gastrocnemius muscle-tendon unit lengths during gait. Gait Posture 90, 464–467. https://doi.org/10.1016/j.gaitpost.2021.09.198.

Cohen, J., 1992. A power primer. Psychol. Bull. 112, 155–159. https://doi.org/10.1016/j.jorganchem.2011.01.025.

Cronin, N.J., Lichtwark, G., 2013. The use of ultrasound to study muscle-tendon function in human posture and locomotion. Gait Posture 37, 305–312.

Dick, T.J.M., Hug, F., 2023. Advances in imaging for assessing the design and mechanics of skeletal muscle in vivo. J. Biomech. 155, 111640 https://doi.org/10.1016/j.jbiomech.2023.111640.

Farris, D.J., Lichtwark, G.A., 2016. UltraTrack: software for semi-automated tracking of muscle fascicles in sequences of B-mode ultrasound images. Comput. Methods Prog. Biomed. 128, 111–118. https://doi.org/10.1016/j.cmpb.2016.02.016.

Ferrari, A., Giovanni, A., Cappello, A., 2010. Gait & Posture Short communication a new formulation of the coefficient of multiple correlation to assess the similarity of waveforms measured synchronously by different motion analysis protocols. Gait Posture 31, 540–542. https://doi.org/10.1016/j.gaitpost.2010.02.009.

Finni, T., Peter, A., Khair, R., Cronin, N.J., 2022. Tendon length estimates are influenced by tracking location. Eur. J. Appl. Physiol. 122, 1857–1862. https://doi.org/10.1007/s00421-022-04958-8.

Fukunaga, T., Kubo, K., Kawakami, Y., Fukashiro, S., Kanehisa, H., Maganaris, C.N., 2001. In vivo behaviour of human muscle tendon during walking. Proc. Biol. Sci. 268, 229–233.

Handsfield, G.G., Williams, S., Khuu, S., Lichtwark, G., Stott, N.S., 2022. Muscle architecture, growth, and biological Remodelling in cerebral palsy: a narrative review. BMC Musculoskelet. Disord. 23, 1–17. https://doi.org/10.1186/s12891-022-05110-5.

Harkness-Armstrong, C., Maganaris, C., Wright, D.M., Bass, A., Baltzopoulos, V., O'Brien, T.D., 2021. Experimental Physiology - 2021 - Harkness-Armstrong - In vivo operating lengths of the gastrocnemius muscle during gait in.pdf.

Horsch, A., Petzinger, L., Ghandour, M., Putz, C., Renkawitz, T., Götze, M., 2022. Defining Equinus foot in cerebral palsy. Children 9. https://doi.org/10.3390/children9070956.

Hösl, M., Böhm, H., Arampatzis, A., Keymer, A., Döderlein, L., 2016. Contractile behavior of the medial gastrocnemius in children with bilateral spastic cerebral palsy during forward, uphill and backward-downhill gait. Clin. Biomech. 36, 32–39. https://doi.org/10.1016/j.clinbiomech.2016.05.008.

Howard, J.J., Graham, K., Shortland, A.P., 2022. Understanding skeletal muscle in cerebral palsy: a path to personalized medicine? Dev. Med. Child Neurol. 64, 289–295. https://doi.org/10.1111/dmcn.15018.

Huang, T.W.P., Shorter, K.A., Adamczyk, P.G., Kuo, A.D., 2015. Mechanical and energetic consequences of reduced ankle plantar-flexion in human walking. J. Exp. Biol. 218, 3541–3550. https://doi.org/10.1242/jeb.113910.

Huijing, P.A., 1999. Muscle as a collagen fiber reinforced composite: a review of force transmission in muscle and whole limb. J. Biomech. 32, 329–345. https://doi.org/10.1016/S0021-9290(98)00186-9.

Ishikawa, M., Komi, P.V., Grey, M.J., Lepola, V., Bruggemann, G.P., 2005. Muscle-tendon interaction and elastic energy usage in human walking. J. Appl. Physiol. 99, 603–608. https://doi.org/10.1152/japplphysiol.00189.2005.

Kadaba, R.W., 2014. Measurement of lower extremity kinematics during level walking. Class. Pap. Orthop. 397–398 https://doi.org/10.1007/978-1-4471-5451-8_100.

Kainz, H., Schwartz, M.H., 2021. The importance of a consistent workflow to estimate muscle-tendon lengths based on joint angles from the conventional gait model. Gait Posture 88, 1–9. https://doi.org/10.1016/j.gaitpost.2021.04.039.

Kalsi, G., Fry, N.R., Shortland, A.P., 2016. Gastrocnemius muscle–tendon interaction during walking in typically-developing adults and children, and in children with spastic cerebral palsy. J. Biomech. 49, 3194–3199. https://doi.org/10.1016/j.jbiomech.2016.07.038.

Kharazi, M., Bohm, S., Theodorakis, C., Mersmann, F., Arampatzis, A., 2021. Quantifying mechanical loading and elastic strain energy of the human Achilles tendon during walking and running. Sci. Rep. 11, 1–13. https://doi.org/10.1038/s41598-021-84847-w.

Leardini, A., Benedetti, M.G., Berti, L., Bettinelli, D., Nativo, R., Giannini, S., 2007. Rear-foot, mid-foot and fore-foot motion during the stance phase of gait. Gait Posture 25, 453–462.

Lee, S.S.M., Gaebler-Spira, D., Zhang, L.Q., Rymer, W.Z., Steele, K.M., 2016. Use of shear wave ultrasound elastography to quantify muscle properties in cerebral palsy. Clin. Biomech. 31, 20–28. https://doi.org/10.1016/j.clinbiomech.2015.10.006.

Lichtwark, G.A., Wilson, A.M., 2006. Interactions between the human gastrocnemius muscle and the Achilles tendon during incline, level and decline locomotion. J. Exp. Biol. 209, 4379–4388.

Lieber, R.L., Fridén, J., 2019. Muscle contracture and passive mechanics in cerebral palsy. J. Appl. Physiol. 126, 1492–1501. https://doi.org/10.1152/japplphysiol.00278.2018.

Monte, A., Tecchio, P., Nardello, F., Bachero-Mena, B., Ardigò, L.P., Zamparo, P., 2022. Influence of muscle-belly and tendon gearing on the energy cost of human walking. Scand. J. Med. Sci. Sports 32, 844–855. https://doi.org/10.1111/sms.14142.

Mooijekind, B., Flux, E., Buizer, A.I., van der Krogt, M.M., Bar-On, L., 2023. The influence of wearing an ultrasound device on gait in children with cerebral palsy and typically developing children. Gait Posture 101, 138–144. https://doi.org/10.1016/j.gaitpost.2023.02.007.

Nikolaou, S., Garcia, M.C., Long, J.T., Allgier, A.J., Goh, Q., Cornwall, R., 2022. Brachial plexus birth injury and cerebral palsy lead to a common contracture phenotype characterized by reduced functional muscle length and strength. Front. Rehabil. Sci. 3, 1–10. https://doi.org/10.3389/fresc.2022.983159.

Orselli, M.I.V., Franz, J.R., Thelen, D.G., Course, E., Hill, C., 2018. Mechanics and energetics in walking. J. Biomech. 60, 227–231. https://doi.org/10.1016/j.jbiomech.2017.06.022.The.

Pataky, T.C., 2012. One-dimensional statistical parametric mapping in Python. Comput. Methods Biomech. Biomed. Engin. 15, 295–301. https://doi.org/10.1080/10255842.2010.527837.

Sawicki, G.S., Lewis, C.L., Ferris, D.P., 2009. It pays to have a spring in your step. Exerc. Sport Sci. Rev. 37, 130–138. https://doi.org/10.1097/JES.0b013e31819c2df6.

Smith, L.R., Lee, K.S., Ward, S.R., Chambers, H.G., Lieber, R.L., 2011. Hamstring contractures in children with spastic cerebral palsy result from a stiffer extracellular matrix and increased in vivo sarcomere length. J. Physiol. 589, 2625–2639. https://doi.org/10.1113/jphysiol.2010.203364.

Stackhouse, Binder-Macleod L., 2005. Voluntary muscle activation, contractile properties, and fatigability in children with and without cerebral palsy, 31, 594–601. https://doi.org/10.1002/mus.20302.VOLUNTARY.

Tecchio, P., Zamparo, P., Nardello, F., Monte, A., 2022. Achilles tendon mechanical properties during walking and running are underestimated when its curvature is not accounted for. J. Biomech. 137 https://doi.org/10.1016/j.jbiomech.2022.111095.

Theis, N., Mohagheghi, A.A., Korff, T., 2016. Mechanical and material properties of the plantarflexor muscles and Achilles tendon in children with spastic cerebral palsy and typically developing children. J. Biomech. 49, 3004–3008.

Valadão, P., Piitulainen, H., Haapala, E.A., Parviainen, T., Avela, J., Finni, T., 2021. Exercise intervention protocol in children and young adults with cerebral palsy: the effects of strength, flexibility and gait training on physical performance, neuromuscular mechanisms and cardiometabolic risk factors (EXECP). BMC Sports Sci. Med. Rehabil. 13, 1–19. https://doi.org/10.1186/s13102-021-00242-y.

Wren, T.A.L., Cheatwood, A.P., Rethlefsen, S.A., Hara, R., Perez, F.J., Kay, R.M., 2010. Achilles tendon length and medial gastrocnemius architecture in children with cerebral palsy and equinus gait. J. Pediatr. Orthop. 30, 479–484.